VIBGYOR ePress

International Journal of Astronautics and Aeronautical Engineering
ISSN: 2631-5009

Heat Transfer Characteristics of Al_2O_3-Kerosene and Fe_3O_4-Kerosene Nanofluids Flowing in a Minitube at Supercritical Pressures

Dan Huang[1*], Xiao-yu Wu[2] and Wei Li[3]

[1]*Department of Mechanical and Electrical Engineering, Central South University of Forestry and Technology, China*

[2]*Department of Mechanical Engineering, Massachusetts Institute of Technology, USA*

[3]*Department of Energy Engineering, Zhejiang University, China*

Abstract

Regenerative cooling system is thought to be an effective and practical solution to better thermal management for high heat flux applications. In this paper, the potential of nanofluids as regenerative coolants at supercritical pressures was evaluated. Two-step method was applied to prepare Al_2O_3-kerosene and Fe_3O_4-kerosene nanofluids. Then experiments were carried out to study the heat transfer characteristics of nanofluids flowing in a vertical minitube at supercritical pressures. Parametric effects of mass flow rate, heat flux, pressure and particle content on the heat transfer performance are presented. Results show that increasing the flow rate or the working pressure could enhance the heat transfer performances, yet higher heat flux leads to poorer heat transfer performances. Besides, the addition of nanoparticles tend to deteriorate heat transfer at supercritical pressures because deposition of the nanoparticles smoothens the wall roughness and presents an additional thermal resistance. As the particle content increases, the heat transfer performance becomes worse.

Keywords

Heat transfer, Supercritical pressure, Parametric effects, Nanofluid

Nomenclature

c: Particle content, wt%; c_p: Specific heat, J/(kg·K); d: Diameter, m; HTC,h: Heat transfer coefficient, W/(m²·K); I: Current, A; L: Length, m; P: Pressure, Pa; Q_m: Mass flow rate, kg/s; Q': Internal heat, W/m³; q: Heat flux, W/m²; R: Radius, m; r: Heat transfer coefficient ratio; T: Temperature, K; U: Voltage, V; x: Distance from the tube inlet, mm

Greek symbols

λ: Thermal conductivity, W/(m·K); μ: Dynamic viscosity, Pa·s; ρ: Density, kg/m³

Subscripts

b: Base fluid; f: Fluid; i: Inner; loss: Heat loss; net: Net; nf: Nanofluid; o: Outer; p: Particle; w: Wall; x: Local value

Introduction

Effective cooling techniques are of great importance in high heat flux applications, such as large parallel computer systems and aircraft combustion chambers. As the temperature and heat load in scramjet applications are very high, effective heat transfer systems and effi-

***Corresponding author:** *Dan Huang, Department of Mechanical and Electrical Engineering, Central South University of Forestry and Technology, Changsha 410004, China, Tel: +86-85623096, Fax: +86-85623038, E-mail: hiwactb@163.com*

Received: November 30, 2017: **Accepted:** March 05, 2018: **Published:** March 07, 2018

Citation: Huang D, Xiao-yu W, Li W (2018) Heat Transfer Characteristics of Al_2O_3-Kerosene and Fe_3O_4-Kerosene Nanofluids Flowing in a Minitube at Supercritical Pressures. Int J Astronaut Aeronautical Eng 3:014

cient coolants are necessary for scramjet engines to survive the extreme heat generated in hypersonic flight. To improve the cooling efficiency of heat transfer systems, the regenerative cooling system, where engine fuel works as a coolant and travels through the cooling tubes along the chamber wall, is developed as an effective thermal management technique [1-3]. Technically, the pressures in scramjet applications are above supercritical pressures and the fuel temperature may also exceed the critical temperature by absorbing heat from the chamber wall. At supercritical pressures, the thermo-physical properties of fuels exhibit extremely rapid variation with temperature, especially near the pseudocritical point, which is quite different from that at subcritical pressures. The unusual variations of the thermo-physical properties of supercritical fuels may enhance the heat transfer significantly and thus have attracted researchers' attention.

Experimental and numerical investigations have been extensively conducted on heat transfer performance of fluids at supercritical pressures, but the previous studies in the open literature are mainly focused on supercritical heat transfer of CO_2 and H_2O [4-8]. Compared to CO_2 and H_2O, the database on the convective heat transfer of hydrocarbon fuels is at a relative small scale [9-11].

A nanofluid is a fluid-solid mixture which is formed by suspending the ultrafine solid nanoparticles (1-100 nm in size) in a base fluid, generally water and oil, etc. Nanofluids have received considerable attention in thermal science and engineering during the last decade [8-10]. By dispersing nanoparticles into hydrocarbon fuel kerosene, the formed nanofluid might be a promising coolant as the nanoparticles can enhance the thermal conductivity of kerosene, especially at high temperatures near the critical point. Since nanofluids are generally thought to have better thermo-physical properties (e.g. higher thermal conductivity [12,13]), nanofluid fuels might be potential regenerative cooling working fluids and might further enhance heat transfer [14-16]. However, few literatures have been published on the studies of supercritical nanofluids. Rahimi [17] adopted a water base Al_2O_3 nanofluid as a coolant in supercritical water reactors. They found that the utilization of nanofluid could enhance the core outlet temperature and increase the heat transfer coefficient in Super-heater zones. Ruan [18] numerically investigated the turbulent heat transfer of a nanofluid, methane-CuO, in a circular cooling tube at supercritical pressures. Their results indicated potential applications of nanofluids in enhancing heat transfer at supercritical pressures.

Under supercritical conditions, the large variation of thermo-physical properties at varying temperatures might lead to interesting thermodynamic and transport properties of nanofluids. Further development of regenerative cooling systems could be derived from supercrit-

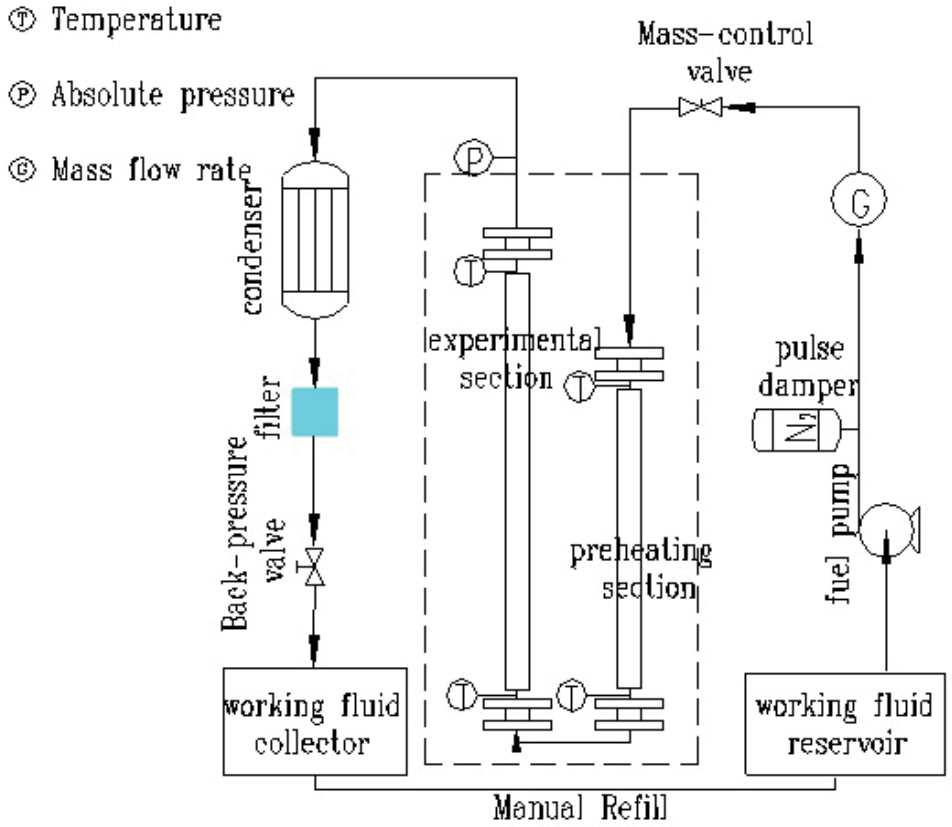

Figure 1: Schematic of the experimental setup.

ical nanofluid studies. Therefore the first attempt was carried out to study heat transfer characteristics of nanofluids at supercritical pressure. In this paper, we prepare stable Al_2O_3-kerosene and Fe_3O_4-kerosene nanofluids and study the heat transfer mechanism of the organic nanofluids under supercritical pressures experimentally. Insights were offered on the effects of the factors such as mass flow rate, pressure, heat flux and particle contents in this work.

Experimental Apparatus

The measured critical pressure and temperature of aviation kerosene are 2.4 MPa and 372.35 °C, respectively. The experimental loop in this paper was constructed to bear high temperature (600 °C) and high pressure (10 MPa), which is schematically introduced in Figure 1.

The nanofluid was circulated and compressed by apiston pump. A pulse damper filled with compressed nitrogen was installed after the pump to reduce the fluctuation of the flow rate. The nanofluid was heated to the required inlet fuel temperature in the preheating section and then sent to the experimental section, being heated and tested at supercritical conditions. After that, the fuel was condensed, recollected and fed into the reservoir manually. The test tube is a vertical stainless steel (1Cr18Ni9Ti) tube with inner diameter (d) of 2.0 mm and outer diameter of 3.0 mm. The heated section of the test tube is 1000 mm long, and the two unheated sections (each with a length of 100 mm, i.e., 50 d) are located before and after the heated section. A low-voltage direct-current power (SKD-60V/120A) was used to heat the test section and simulate constant heat flux condition. The inlet and outlet temperatures of the test section were carefully obtained using armored K-type thermocouples. The local wall temperatures of the test section were measured by twelve K-type thermocouples (φ 0.3 mm),which were carefully welded onto but insulated with the tube outer surface. Details of the control parameters and operation of the experimental loop were given in Ref. [19].

A two-step method was applied to prepare Al_2O_3-kerosene and Fe_3O_4-kerosene nanofluids. Aviation kerosene was used as the base fluid, and the Al_2O_3 and Fe_3O_4 particles were surface-modified by oleic acid to improve dispersion stability. The dispersion was mixed by an electric stirrer for 30 minutes, followed by ultrasonic oscillation for 45 minutes. After the mixing, the nanoparticle size in nanofluids was measured by a MALVERN ZETASIZER NANO 590. The average nanoparticle size for Al_2O_3-kerosene nanofluid is 403.9 nm and for Fe_3O_4-kerosene nanofluid is 148.5 nm. A sample of the nanofluid was settled aside after the mixing. Marginal sedimentation in the prepared Al_2O_3-kerosene and Fe_3O_4-kerosene nanofluids was noticed after more than two months. Besides, experiments were conducted within two days after the nanofluid preparation.

Data Reduction

The local inner wall temperature, $T_{wi,x}$, can be deduced from the outer wall temperature ($T_{wo,x}$) by assuming one-dimensional heat conduction with an internal heat source (Q')as:

$$T_{wi,x} = T_{wo,x} + \frac{1}{4}\frac{Q'}{\lambda}\left(R_o^2 - R_i^2\right) + \frac{1}{2}\frac{Q'}{\lambda}R_o^2 \ln\frac{R_i}{R_o} \quad (1)$$

The local heat transfer coefficient (HTC) along the tube length can be calculated by the following equation:

$$h_x = \frac{q_{net}}{T_{wi,x} - T_{f,x}} \quad (2)$$

Where $T_{f,x}$ is the local fuel temperature and can be calculated from the local enthalpy, heat flux and mass flow rate; q_{net} is the net heat flux and can be calculated by:

$$q_{net} = q_x - q_{loss} = \frac{UI}{\pi D_i L} - q_{loss} \quad (3)$$

Where q_x is the total heat flux, q_{loss} is the heat loss at the test section, which was obtained experimentally. The tube was wrapped with insulation first; then by varying the heating power, the outer wall temperature of the tube became stable after a certain amount of time when there was no flowing fluid through it. At steady state, the heating power input into the tube was considered to be almost the same as the heat loss at a certain tube outer temperature. Thus, by plotting the relationship between the heating power and the outer wall temperature, the heat loss at different outer tube wall temperatures could be identified by interpolation from the figure. q_{loss} was founded to be less than 5% of the electric power input to the test section. The relative errors for measurement and accumulated errors by calculations are listed in Table 1.

At supercritical conditions, the thermo-physical properties of the hydrocarbon fuel mixture undergo strong variations. Thus it is very important to accurately predict the property variations with temperature. The density, specific heat, thermal conductivity and viscosity of the aviation kerosene at various temperatures were obtained by a 10-species surrogate proposed by Zhong, et al. [1] and the NIST Supertrapp software [20-22]. The

Table 1: Error analysis.

Item	Error (%)
Temperature	0.78
Pressure	0.36
Mass flow rate	1.67
Heat flux	2.36
Heat transfer coefficient	2.6

Table 2: Thermo-physical properties of particle and nanofluid.

	Al_2O_3	Fe_3O_4
ρ_p	3970	5100
$c_{p,p}$	102.429 + 38.7498T/1000-15.9109(T/1000)^2 + 2.628181(T/1000)^3 - 3.00755/(T/1000)^2	104.2096 + 178.5108T/1000-10.6151(T/1000)^2 + 1.132534(T/1000)^3 – 0.9942/(T/1000)^2
λ_p	9*10^{-5} T^2 - 0.1426T + 69.117	
ρ_{nf}	(1- ϕ_p) ρ_f + $\phi_p\rho_p$	
$c_{p,nf}$	((1- ϕ_p) ρ_f $c_{p,f}$ + $\phi_p\rho_p c_{p,p}$)/ρ_{nf}	
μ_{nf}	(1 + 2.5 ϕ_p)μ_f	
λ_{nf}	(λ_p+(n-1) λ_f + (n-1) ϕ_p(λ_p-λ_f))λ_f/(λ_p+ (n-1) λ_f - ϕ_p(λ_p - λ_f))	

Note: n = 3 for spherical particles.

Table 3: Operating parameters.

Direction	Pressure	Mass flow rate	Operating heat flux	Nanoparticle contents
Upward	3-4.5 MPa	2-3.5 g/s	190-300 kW/m^2	0.02-0.1 wt.%

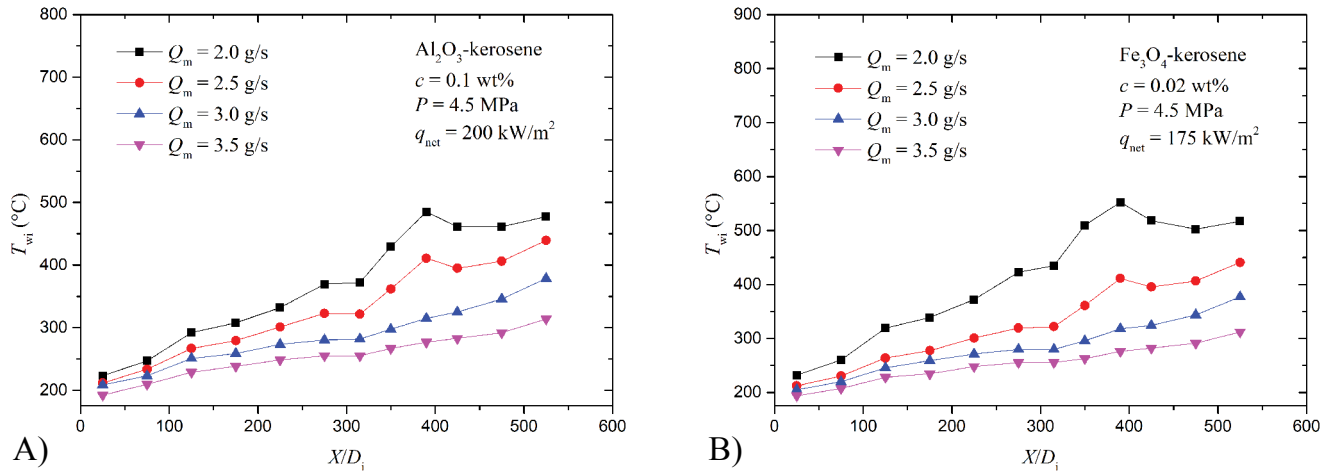

Figure 2: The local wall temperature distributions along tube length: a) Al_2O_3-kerosene nanofluid; b) Fe_3O_4-kerosene nanofluid.

comparison of numerical data and experimental data [23-26] for the thermo-physical properties of aviation kerosene at P = 3 Mpa can be found in our previous publication [27]. Good agreement has been reached between the calculated results and experimental data.

Based on the homogeneous mixture model and heat transfer of the diluted nanofluids [28,29], the following expressions, as shown in Table 2, are used to calculate density, specific heat and thermal conductivity of the Al_2O_3 and Fe_3O_4 particles and nanofluid. The nanofluid properties can be predicted by the nanofluid correlation listed in Table 2, especially at very small volume content (about 0.02 vol.%).

Table 3 briefly summarizes the operating conditions for all experiments.

Results and Discussion

Effects of mass flow rate

The mass flow rate is an important factor that influences the heat transfer performance at supercritical pressures, as the turbulence and boundary layer will be affected by the varying flow rate. The effects of mass flow rate on heat transfer can be seen from Figure 2 and Figure 3. Figures show that the local wall temperature basically increases along the tube length at different mass flow rate, while the heat transfer coefficient first increases to a maximum value and then continuously decreases.

By inspecting Figure 4 carefully, we can divide the experimental section into three zones along the tube length at supercritical pressures:

1. Inlet zone, where the tube wall temperatures are lower than supercritical temperature. In this zone, the heat transfer mechanism could be identified as convective flow. As the local wall temperature and fluid temperature are relatively low, not large enough to significantly affect the thermo-physical properties, the variations of the local wall temperature and heat transfer coefficient are small and they both increase along the tube.
2. Middle zone, where the tube wall temperature is higher than the supercritical temperature. As the near wall fluid has very low density and low viscosity,

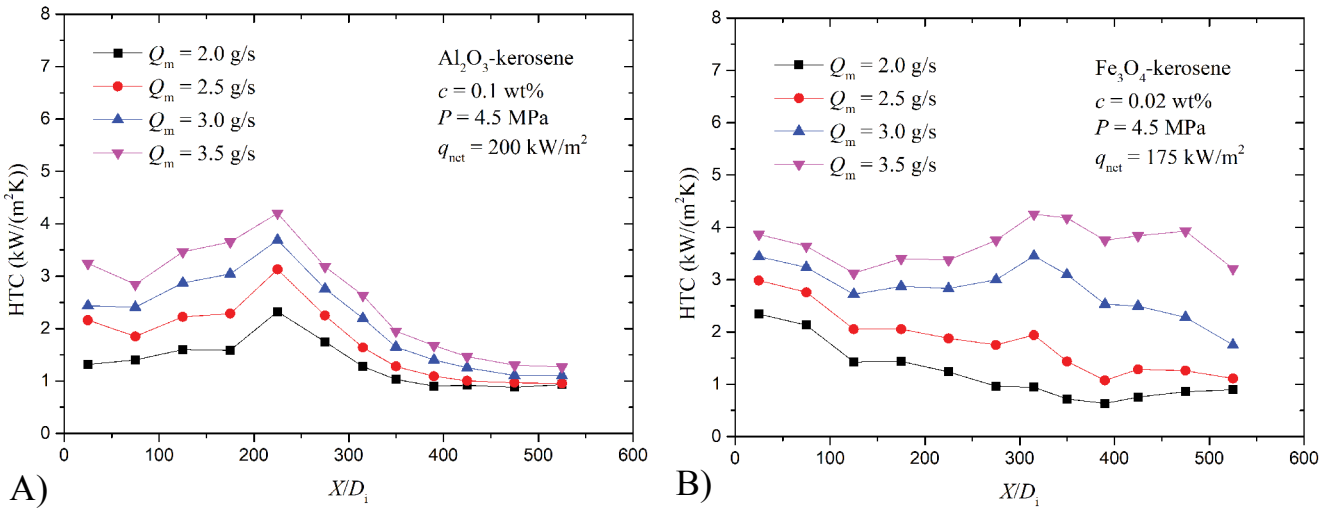

Figure 3: Heat transfer coefficient distributions along tube length: a) Al_2O_3-kerosene nanofluid; b) Fe_3O_4-kerosene nanofluid.

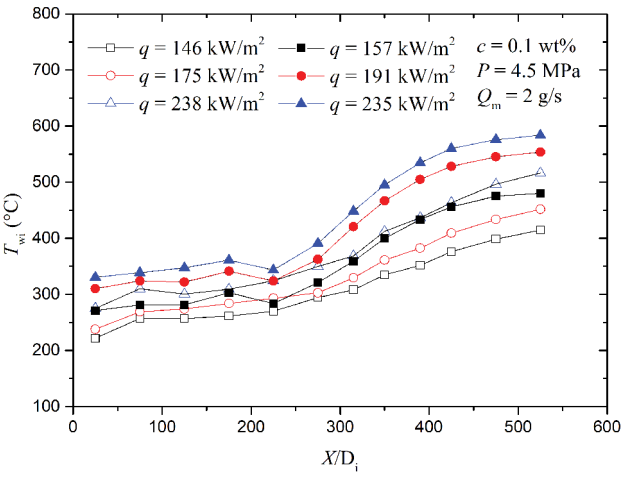

Figure 4: T_{wi} of Al_2O_3-kerosene nanofluid (solid symbols) and kerosene (hollow symbols) distributions along tube length.

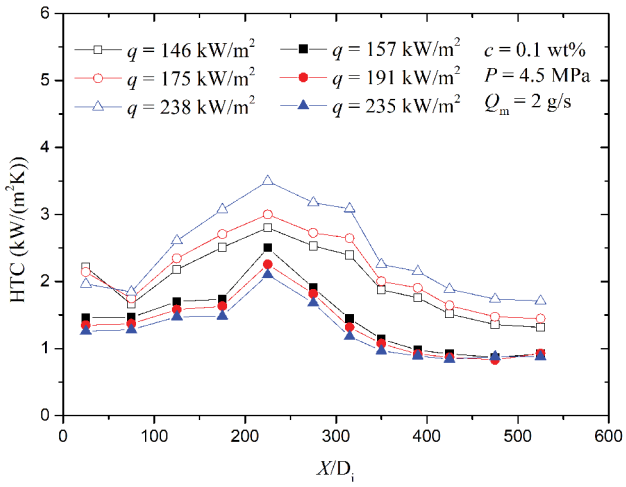

Figure 5: HTC of Al_2O_3-kerosene nanofluid (solid symbols) and kerosene (hollow symbols) distributions along tube length.

a film-like fluid will embrace the fluid in center and become a barrier with high thermal resistance for the heat transfer between the bulk flow and the tube wall. Thus, this type of pseudo-film flow deteriorates heat transfer performances. Besides, the density and viscosity of the near wall fluid are both lower than those of the fluid in center, so the nanoparticles will be kept at fluid in center. Thus, the nanoparticles could not enhance heat transfer performances at this zone and the local wall temperature increases and the corresponding heat transfer coefficient decreases.

3. Outlet zone, where the local wall temperature is above the pseudocritical temperature. In this zone, the specific heat of the fluid near the wall maintains a high value and the thermal conductivity begins to increase. These two factors suppress the heat transfer deterioration. Thus the variations of the local wall temperature and heat transfer coefficient become gentle again.

Effects of heat flux

As the heat flux may influence the changes of fluid temperature and wall temperature, while the variation of fluid temperature and wall temperature will affect the variation of thermo-physical properties, the heat flux might have significant influence on the heat transfer of nanofluid.

Figure 4 and Figure 5 show the wall temperature and HTC distributions of Al_2O_3-kerosene nanofluid. From the figures, we know that smaller heat flux leads to better heat transfer performances of nanofluids. As the bulk fluid temperature increases, the specific heat will increase while the viscosity and density will both decrease. Thus, heat transfer performances will be enhanced by hotter bulk fluids. However on the other hand, as shown in Figure 4, when the heat flux is higher, the local inner tube wall temperature is also higher. Hotter tube wall,

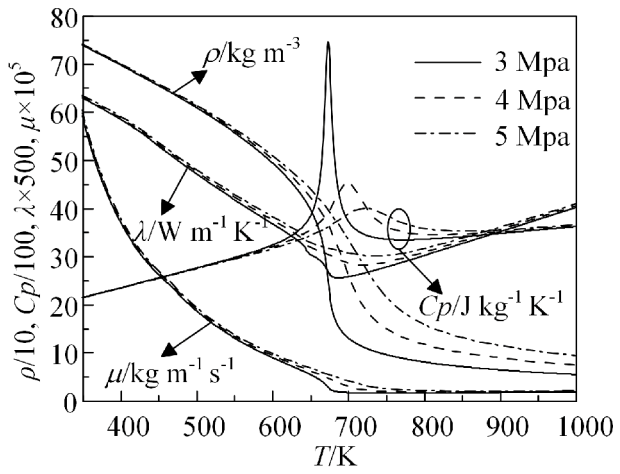

Figure 6: Variation of the kerosene properties with temperature (P = 3, 4 and 5 MPa).

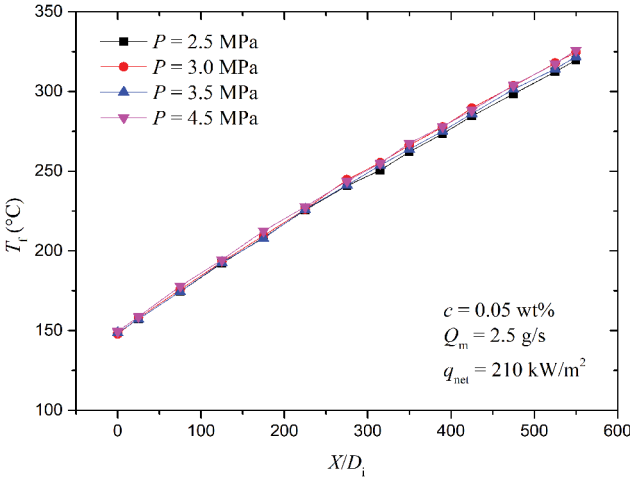

Figure 8: T_f of Fe_3O_4-kerosene nanofluid distributions along tube length.

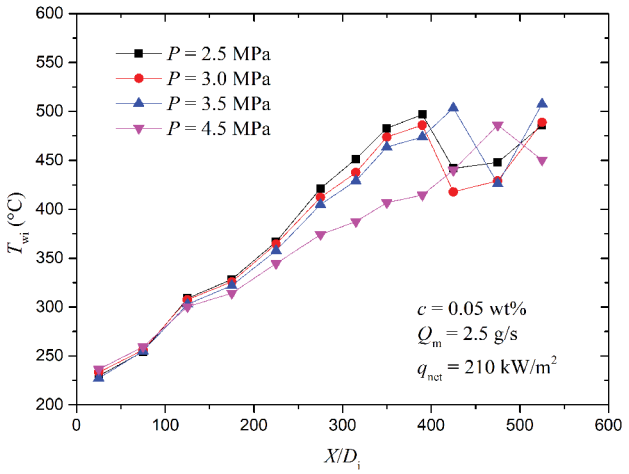

Figure 7: T_{wi} of Fe_3O_4-kerosene nanofluid distributions along tube length.

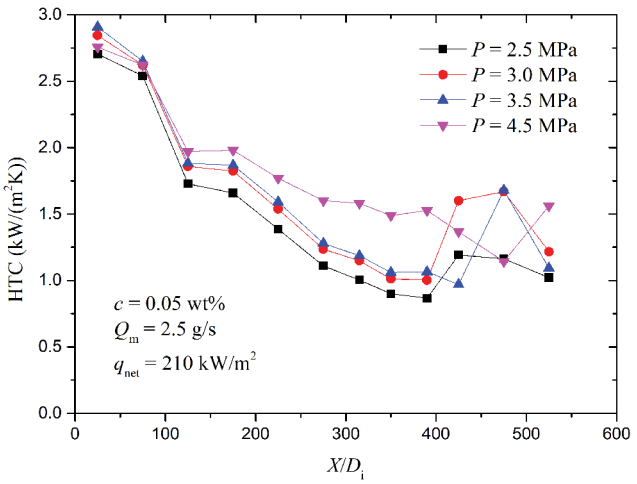

Figure 9: HTC of Fe_3O_4-kerosene nanofluid distributions along tube length.

which is caused by higher heat flux, provokes severer pseudo-film flow near the tube wall, so the heat transfer performances will be worse. Thus, heat flux has intriguing effects on heat transfer performances of nanofluids at supercritical pressures. At the current situation, though not shown here, the bulk fluid temperatures are all below the supercritical temperature, so the heat transfer enhancement caused by variations of thermo-physical properties near the supercritical point has not induced in these cases. Therefore, the heat transfer deterioration effects of pseudo-film flow overcome the heat transfer enhancement of hotter fluids and the heat transfer coefficients decrease by increasing heat flux.

The local wall temperature and HTC of the base fluid (kerosene, hollow symbols) are also presented in Figure 4 and Figure 5. It can be seen that the Al_2O_3-kerosene nanofluids have higher wall temperature and lower HTC values than that of kerosene at the same working conditions, which means that the base fluid has better heat transfer performance than the Al_2O_3-kerosene nanofluid. This might be due to the inner tube wall modification by nanoparticle depositions. Details of the comparison between the base fluid and the nanofluids will be presented in Section 4.4.

Effects of pressure

From the thermo-physical properties of kerosene as shown in Figure 6, it is obvious that when the temperature of the kerosene is lower than the critical temperature, pressure has a relatively small effect on density, viscosity and thermal conductivity. However, at temperatures higher than the supercritical temperature, pressure tends to present strong effects on the thermo-physical properties. The changes in thermo-physical properties affect accordingly the heat transfer performance, similar as above. Figure 7 and Figure 8 show the local wall temperature and fluid temperature distributions of Fe_3O_4-kerosene nanofluid along the tube length at pressures ranging from 2.5 to 4.5 MPa.

From the figures, we know that at different working pressure, if the heat fluxes and flow rates are the same, the local wall temperature and fluid temperature are almost the same when the they are both lower than the critical temperature. When the local wall temperature is higher than the critical temperature, increasing pressure causes a decrease in the local wall temperature.

Figure 9 depicts the local HTC distributions along the tube at different working pressures. The local HTC increases as pressure increases, especially when the pressure (i.e., 4.5 MPa) is much larger than the critical pressure. The reasons lie in the changes of the thermo-physical properties of kerosene at different pressures. As shown in Figure 6, the variations of density and heat capacity are much smoother at 4.5 MPa and the heat capacity increases as pressure increases. The larger thermal conductivity and heat capacity at higher pressures enhance the heat transfer. Besides, the viscosity and density both increase with increasing pressures, thus the pseudo-film flow would be suppressed at higher pressures and the nanofluids could have better heat transfer performances. Consequently the heat transfer coefficient is higher at higher working pressures.

Effects of particle content

In order to study the heat transfer performances of nanofluids at supercritical pressure, a heat transfer coefficient ratio is defined as follows to compare the heat transfer coefficients of nanofluids and those of base fluid under the same working conditions:

$$r = \frac{h_{nf}}{h_b} \quad (1)$$

The comparisons between heat transfer coefficients of Al_2O_3-kerosene and Fe_3O_4-kerosene nanofluids with different particle content and those of the base fluid (kerosene) at the same working conditions are shown in Figure 10. We could see that most of the data points are under the dotted line of 1.0, which means that nanofluids have lower heat transfer coefficients than the base fluid and the nanofluids tend to deteriorate the heat transfer performance at supercritical pressures. Besides, the 0.1 wt% nanofluids have the smallest heat transfer ratios while the ratios of 0.02 wt% nanofluids are closest to the 1.0 dotted line. Thus, we conclude that nanofluids have poorer heat transfer performances than the base fluid at supercritical pressures, and higher particle contents leads to worse heat transfer performances.

The heat transfer deterioration effects of nanofluids might be caused by the modification of inner tube wall surfaces by nanoparticles precipitations. At supercritical conditions, the viscosity and density of the base fluids are both very low, so the base fluid might not be able to hold the nanoparticles. In addition, the decrease in viscosity leads to strong turbulence and thus the nanoparticles move violently. These two factors lead to the deposition of nanoparticles on the inner tube wall surfaces and thus deteriorate the heat transfer performance. A Scanning Electron Microscope (SEM) as shown in Figure 11, was used to identify the modifications of the inner wall surface by nanofluids. It was found that there exist many bulges on the inner surface before experiments. However, after the nanofluid heat transfer experiments, the bulges disappeared and the surface became smoother. Besides the additional thermal resistance caused by the nanoparticle deposit layer, roughness effects of the bulges might be suppressed in the smoother tube. Thus the HTC of Al_2O_3-kerosene and Fe_3O_4-kerosene nanofluids tends to be lower than that of pure kerosene. However, further investigations should be performed to identify

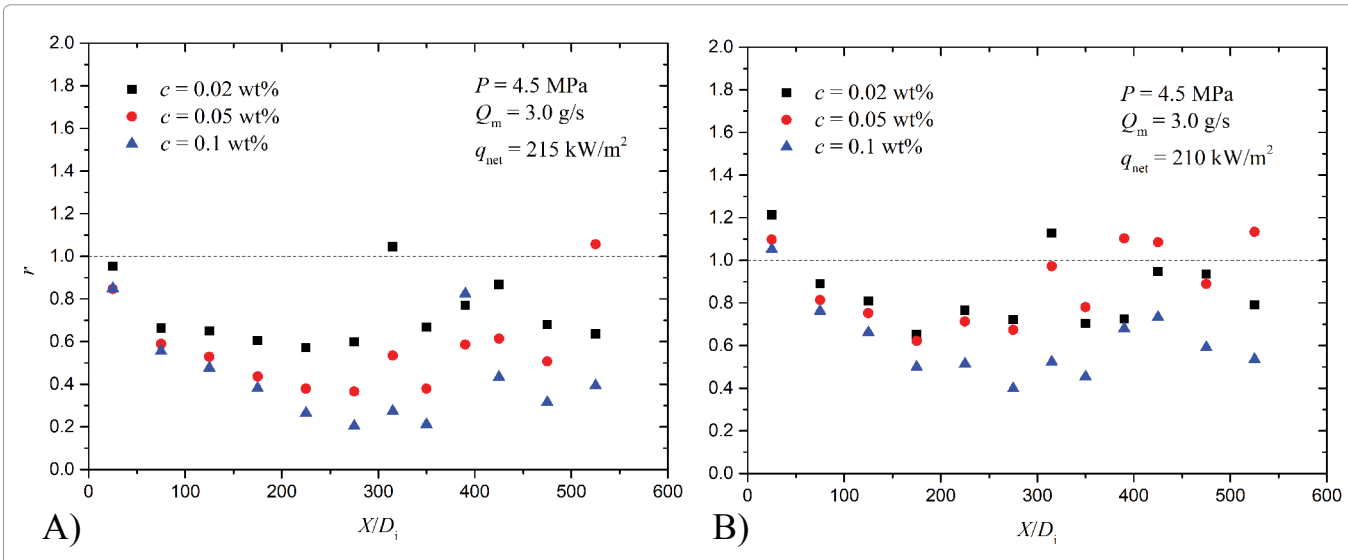

Figure 10: Heat transfer ratios of nanofluids at supercritical pressure: a) Al_2O_3-kerosene nanofluid; b) Fe_3O_4-kerosene nanofluid.

Citation: Huang D, Xiao-yu W, Li W (2018) Heat Transfer Characteristics of Al_2O_3-Kerosene and Fe_3O_4-Kerosene Nanofluids Flowing in a Minitube at Supercritical Pressures. Int J Astronaut Aeronautical Eng 3:014

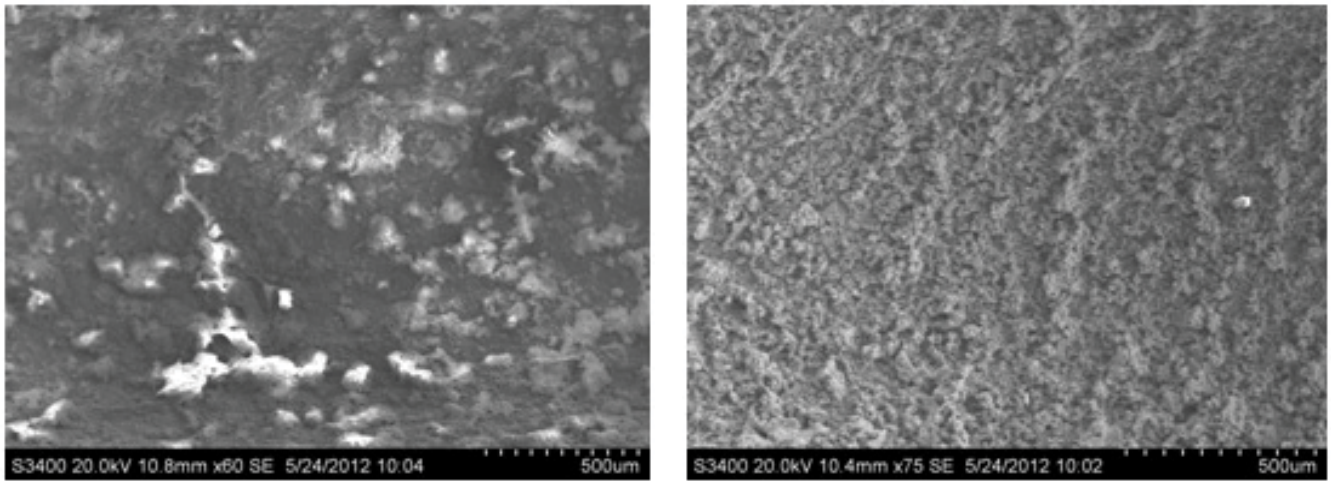

Figure 11: SEM pictures of inner tube wall surfaces a) Tube wall surface before nanofluids experiments; b) Tube wall surface after nanofluids experiments.

the modified characteristics of different particle materials on different tube wall materials at supercritical conditions. Also the compatibility between nanoparticles and tube materials should be considered for development of nanofluids as regenerative coolants.

Conclusions

Experiments were performed to investigate the heat transfer performance of Al_2O_3-kerosene and Fe_3O_4-kerosene nanofluids at supercritical pressures. Parametric effects of mass flow rate, pressure, heat flux and particle content were studied specifically. The main results from this work are summarized as follows:

1. At supercritical pressure, the experimental section can be divided into three zones: inlet-, middle- and outlet-zones under various mass flow rates. At the inlet zone, the convective flow heat transfer mechanism dominated, and the local wall temperature and heat transfer coefficients both increase along the tube. At the middle zone, nanofluids are under pseudo-film flow mechanism, thus the heat transfer coefficient drops. At the outlet zone, the variation of the local wall temperature and heat transfer coefficient become gentle again. Increasing mass flow rate could enhance the heat transfer performance of nanofluids flowing in a vertical tube under supercritical pressure.
2. The effects of heat flux on heat transfer are complicated. The heat transfer deterioration effect of severer pseudo-film flow will compete with the enhancement effect of hotter bulk fluid with higher specific heat. In our experiments, the heat transfer deterioration effect stands out, so higher heat flux leads to poorer heat transfer performances of nanofluids.
3. Working pressure affects the heat transfer performance when the inner wall temperature is higher than the critical temperature. As higher pressure will restrain the film-like flow near the tube wall, the heat transfer performances at higher pressure will be better.
4. The addition of nanoparticles deteriorates the heat transfer performance of Al_2O_3-kerosene and Fe_3O_4-kerosene nanofluids at supercritical pressures. As the particle content increases, the heat transfer coefficient decreases due to the modification of the inner wall surface by the nanoparticles.

Acknowledgements

This work is supported by the Scientific Research Foundation for Talented Scholars of CSUFT University (2016YJ002) and China Postdoctoral Science Foundation (2017M612603).

References

1. F Zhong, X Fan, G Yu, J Li, CJ Sung (2009) Heat transfer of aviation kerosene at supercritical conditions. J Thermophys Heat Transfer 23: 543-550.
2. H Huang, LJ Spadaccini, DR Sobel (2004) Fuel-cooled thermal management for advanced aeroengines. J Eng Gas Turb Power 126: 284-293.
3. CN Sokmen (2011) Effect of property variations on the mixing of laminar supercritical water streams in a T-junction. Int Commun Heat Mass Transfer 38: 85-92.
4. Wang H, Bi QC, Yang ZD, Wang LC (2015) Experimental and numerical investigation of heat transfer from a narrow annulus to supercritical pressure water. Ann Nucl Energ 80: 416-428.
5. Gang W, Pan J, Bi QC, Yang ZD, Wang H (2014) Heat transfer characteristics of supercritical pressure water in vertical upward annuli. Nucl Eng Des 273: 449-458.
6. Shen Z, Yang D, Chen GM, Xiao F (2014) Experimental investigation on heat transfer characteristics of smooth tube with downward flow. Int J Heat Mass Transfer 68: 669-676.

7. Jiang PX, Liu B, Zhao CR, Luo F (2013) Convection heat transfer of supercritical pressure carbon dioxide in a vertical micro tube from transition to turbulent flow regime. Int J Heat Mass Transfer 56: 741-749.

8. Kim DE, Kim MH (2011) Experimental investigation of heat transfer in vertical upward and downward supercritical CO_2 flow in a circular tube. Int J Heat Fluid Flow 32: 176-191.

9. Zhu JQ, Tao Z, Deng HW, Wang K, Yu X (2015) Numerical investigation of heat transfer characteristics and flow resistance of kerosene RP-3 under supercritical pressure. Int J Heat Mass Transfer 91: 330-341.

10. Li W, Huang D, Xu GQ, Tao Z, Zan W, et al. (2015) Heat transfer to aviation kerosene flowing upward in smooth tubes at supercritical pressures. Int J Heat Mass Transfer 85: 1084-1094.

11. Xu KK, Tang LJ, Meng H (2015) Numerical study of supercritical-pressure fluid flows and heat transfer of methane in ribbed cooling tubes. Int J Heat Mass Transfer 84: 346-358.

12. C Selvam, D Mohan Lal, Sivasankaran Harish (2016) Thermophysical properties of ethylene glycol-water mixture containing silver nanoparticles. J Mech Sci Tech 30: 1271-1279.

13. C Selvam, EC Muhammed Irshad, D Mohan Lal, Sivasankaran Harish (2016) Convective heat transfer characteristics of water-ethylene glycol mixture with silver nanoparticles. Exp Therm Fluid Sci 77: 188-196.

14. Hu YW, He YR, Qi C, Jiang BC, Schlaberg HI (2014) Experimental and numerical study of natural convection in a square enclosure filled with nanofluid. Int J Heat Mass Transfer 78: 380-392.

15. Zhang J, Diao YH, Zhao YH, Zhang YN (2014) Experimental study of TiO_2-water nanofluid flow and heat transfer characteristics in a multiport minichannel flat tube. Int J Heat Mass Transfer 79: 628-638.

16. Ryzhkov II, Minakov AV (2014) The effect of nanoparticle diffusion and thermophoresis on convective heat transfer of nanofluid in a circular tube. Int J Heat Mass Transfer 77: 956-969.

17. MH Rahimi, G Jahanfarnia, N Vosoughi (2017) Thermal-hydrulic analysis of nanofluids as the coolant in supercritical water reactors. J Super Fluids 128: 47-56.

18. B Ruan, X Gao, H Meng (2017) Numerical modeling of turbulent heat transfer of a nanofluid at supercritical pressure. Appl Therm Eng 113: 994-1003.

19. Huang D, Ruan B, Wu XY, Zhang W, Xu GQ, et al. (2015) Experimental study on heat transfer of aviation kerosene in a vertical upward tube at supercritical pressures. Chinese J Chem Eng 23: 425-434.

20. Ely JF, Hanley H (1981) Prediction of transport properties. 1. Viscosity of fluids and mixtures. Ind Eng Chem Fundam 20: 323-332.

21. Ely JF, Hanley H (1983) Prediction of transport properties. 2. Thermal conductivity of pure fluids and mixtures. Ind Eng Chem Fundam 22: 90-97.

22. Meng H, Yang V (2003) A unified treatment of general fluid thermodynamics and its application to a preconditioning scheme. J Comput Phys 189: 277-304.

23. Deng HW, Zhu K, Xu GQ, Tao Z, Zhang CB (2012) Isobaric specific heat capacity measurement for kerosene RP-3 in the near-critical and supercritical regions. J Chem Eng Data 57: 263-268.

24. Xu GQ, Jia ZX, Wen J, Deng HW, Fu YC (2015) Thermal-conductivity measurement of aviation kerosene RP-3 from (285 to 513) K at sub- and supercritical pressures. Int J Thermophys 36: 620-632.

25. Deng HW, Zhang CB, Xu GQ, Tao Z, Zhang B, et al. (2011) Density measurements of endothermic hydrocarbon fuel at sub- and supercritical conditions. J Chem Eng Data 56: 2980-2986.

26. Deng HW, Zhang CB, Xu GQ, Zhang B, Tao Z, et al. (2012) Viscosity measurements of endothermic hydrocarbon fuel from (298 to 788) K under supercritical pressure conditions. J Chem Eng Data 57: 358-365.

27. D Huang, W Li (2017) Heat transfer deterioration of aviation kerosene flowing in mini tubes at supercritical pressures. Int J Heat Mass Transfer 111: 266-278.

28. Y Xuan, W Roetzel (2000) Conceptions for heat transfer correlation of nanofluids. Int J Heat Mass Transfer 43: 3701-3707.

29. A Kamyar, R Saidur, M Hasanuzzaman (2012) Application of computational fluid dynamics (CFD) for nanofluid. Int J Heat Mass Transfer 55: 4104-4115.

Citation: Huang D, Xiao-yu W, Li W (2018) Heat Transfer Characteristics of Al_2O_3-Kerosene and Fe_3O_4-Kerosene Nanofluids Flowing in a Minitube at Supercritical Pressures. Int J Astronaut Aeronautical Eng 3:014